

Radiative transitions of low-lying positive-parity mesons*

John Babcock and Jonathan L. Rosner

School of Physics and Astronomy, University of Minnesota, Minneapolis, Minnesota 55455

(Received 12 April 1976)

Experiments soon to be performed, such as Coulomb dissociation of hadrons and $e^+e^- \rightarrow e^+e^- + \text{hadrons}$, will be able to measure radiative decays of mesons with $J^{PC} = 2^{++}, 1^{++}, 0^{++}$, and 1^{+-} . In advance of these experiments, predictions are made for rates and angular distributions in such processes as $A_{1,2} \rightarrow \pi\gamma$, $f_0 \rightarrow \rho\gamma$, and $f_0 \rightarrow \gamma\gamma$. These predictions are based only on vector dominance and single-quark selection rules, but will permit the first tests of such hypotheses for excited mesons. Results include: (a) relatively large partial widths for $f_0 \rightarrow \gamma\rho$ and $f_0 \rightarrow \gamma\gamma$: $\Gamma(f_0 \rightarrow \gamma\rho) \simeq 1.5 \text{ MeV}$ and $\Gamma(f_0 \rightarrow \gamma\gamma) \simeq 8 \text{ keV}$; (b) the suppression of $\lambda = 0, \pm 1$ decays relative to $\lambda = \pm 2$ for these processes; (c) relative phases for helicity amplitudes in these processes, implying definite angular distributions in $\gamma\gamma \rightarrow f_0 \rightarrow \pi\pi$ and $f_0 \rightarrow \gamma\rho \rightarrow \gamma\pi^+\pi^-$; and (d) the nearly complete suppression of $\gamma\gamma$ couplings of $0^{++} q\bar{q}$ states.

I. INTRODUCTION

In the past two years many heavy narrow meson resonances have been discovered, largely through their coupling to photons. For some fortunate reason, possibly because they contain new constituents, these mesons couple less strongly to the ordinary hadrons than one might have expected. The new heavy mesons thus are an ideal testing ground for theories of electromagnetic transitions of hadrons.

Models of one- and two-photon emission by hadrons often rely on explicit quark descriptions. These models are highly predictive, correlating a wide range of transition matrix elements with one another. However, when the numerical predictions fail it is often hard to see any consistent pattern in the failure.

A less ambitious approach is to abstract symmetries from quark models and to test these symmetries first. As regards transitions, these symmetries have a simple physical interpretation: If they are valid, it appears that a single quark participates in pion or photon emission. The most elegant statement of this assumption is contained in the work of Melosh.¹

The single-quark-transition assumption has been shown to be consistent with data in a wide variety of cases.²⁻⁴ Of course, it is always of interest to see how widespread its validity might be. Recently, with the additional help of the vector-dominance hypothesis, we have extended the single-quark description to make a number of predictions about the electromagnetic decays of the new mesons.⁵ Further implications of these predictions have been discussed in Ref. 6. The strongest predictions deal with the electromagnetic decays of the new candidates for $q\bar{q}$, $L=1$ mesons.

In order to test the underpinnings of the above

calculations, it would be very helpful to test the single-quark-transition and vector-dominance assumptions for electromagnetic transitions of the "old" $q\bar{q}$ $L=1$ mesons: the f_0 , A_2 , A_1 , B , δ , and others below 1.5 GeV. These mesons tend to have large hadronic widths, so that the electromagnetic branching ratios are small. Fortunately, there are specific experiments sensitive to the electromagnetic processes. The decay width of $A_2 \rightarrow \pi\gamma$ can be measured by exciting the pion to an A_2 in the Coulomb field of a nucleus.⁷ A forthcoming experiment at Fermilab⁸ will use this method. The "two-photon" process in $e^+e^- \rightarrow e^+e^- + \text{hadrons}$ can be used to produce the f_0 ,⁹ and will be studied shortly at SPEAR.¹⁰ Finally, some processes are expected to be relatively prominent despite the fact that they are electromagnetic: $f_0 \rightarrow \gamma\rho$ is one of these. The use of track-sensitive targets and other devices to detect single photons may make this mode easier to study than in the past. Many radiative transitions of the positive-parity mesons are likely to be measured in the next year or two, and they will be of some theoretical interest for the reasons mentioned above. Consequently, we have prepared a brief summary of the electromagnetic decay widths and helicity amplitudes for the best-studied positive-parity mesons. [Further predictions may be made with the help of U(3) invariance.] Our approach is primarily to provide a guide to "interesting" experiments. One point of more theoretical interest is that *the processes mentioned here are the first nontrivial ones where the single-quark (Melosh-transformation) descriptions of pion emission and photon emission overlap*. By demanding consistency of two ways of describing the decays $A_2 \rightarrow \gamma\pi$, $A_1 \rightarrow \gamma\pi$, and $B \rightarrow \gamma\pi$, we obtain powerful constraints,¹¹ which can then be tested in such processes as $f_0 \rightarrow \gamma\rho$, $f_0 \rightarrow \gamma\gamma$, and $(0^{++}) \rightarrow \gamma\gamma$. We shall indicate specific ways of testing these con-

straints.

In Sec. II we review notation and give expressions for transition matrix elements to γ + meson and $\gamma + \gamma$. In Sec. III we endow these expressions with numerical values by using vector dominance, thus predicting both partial widths and individual decay helicity amplitudes. Section IV deals with concrete experimental tests of these predictions in hadron, photon, and colliding lepton beams. It contains explicit predictions of cross sections and angular distributions. Section V contains a summary and conclusions. An appendix deals with angular correlations in $\gamma\gamma \rightarrow \mu^+ \mu^-$, a useful "calibration" process.

II. NOTATION AND MATRIX ELEMENTS

The single-quark selection rules for on-shell couplings of pions and photons are conveniently described with the help of the Melosh transformation.¹ Helicity amplitudes for single-pion and single-photon emission are proportional to the matrix elements of the lightlike axial charge Q_5 and the lightlike dipole operator D_+ , respectively. Both Q_5 and D_+ have simple transformation properties under an $SU(6)_W$ algebra of currents: Q_5 transforms as

$$Q_5 \propto \underline{35}(8, 3)_0, \quad \Delta L_z = 0, \quad (1)$$

while D_+ transforms as

$$D_+ \propto \underline{35}(8, 1)_0, \quad \Delta L_z = 1. \quad (2)$$

Here we have used the notation²⁻⁴

$$\underline{SU(6)}_W(SU(3), SU(2))_{\Delta W_z, \Delta L_z}. \quad (3)$$

While hadrons seem to fall into irreducible multiplets of an $SU(6)_W \times O(3)$ "constituents" algebra, there are sound theoretical and experimental reasons for believing that the $SU(6)_W$ "constituents" algebra is not the same as the $SU(6)_W$ "currents" algebra. Melosh postulated that a unitary transformation V connects the two algebras:

$$\begin{aligned} |\text{hadron}\rangle &= |\text{I.R., constituents}\rangle \\ &= V |\text{I.R., currents}\rangle. \end{aligned} \quad (4)$$

Then the matrix elements of interest are

$$\begin{aligned} \langle \text{hadron}' | (Q_5 \text{ or } D_+) | \text{hadron}\rangle \\ = \langle \text{I.R.}', \text{currents} | V^+ (Q_5 \text{ or } D_+) V | \text{I.R., currents}\rangle. \end{aligned} \quad (5)$$

Melosh noted that in the free-quark model the transformed charges $\tilde{Q}_5 \equiv V^+ Q_5 V$ and $\tilde{D}_+ \equiv V^+ D_+ V$ still have relatively simple transformation properties under the $SU(6)_W$ "currents" algebra, namely,

$$\begin{aligned} \tilde{Q}_5 &\propto \underline{35}(8, 3)_0, \Delta L_z = 0 \quad (\text{a}) \\ &+ \underline{35}(8, 3)_{\mp 1}, \Delta L_z = \pm 1, \quad (\text{b}) \end{aligned} \quad (6)$$

$$\begin{aligned} \tilde{D}_+ &\propto \underline{35}(8, 1)_0, \Delta L_z = 1 \quad [D(0, 0)] \\ &+ \underline{35}(8, 3)_1, \Delta L_z = 0 \quad [D(1, 1)] \\ &+ \underline{35}(8, 3)_0, \Delta L_z = 1 \quad [D(1, 0)] \\ &+ \underline{35}(8, 3)_{-1}, \Delta L_z = 2 \quad [D(1, -1)]. \end{aligned} \quad (7)$$

Here the quantities in parentheses on the right label reduced matrix elements; the labels in Eq. (7) correspond to $D(W, W_z)$. The reduced matrix elements are free parameters, distinct for each pair of $SU(6) \times O(3)$ multiplets. We shall be concentrating on the processes

$$\underline{35}, L = 1 \rightarrow (\pi \text{ or } \gamma) + \underline{35}, L = 0 \quad (8)$$

in this paper.

One should note that in Eqs. (6) and (7) the Melosh transformation has generated all of the single-quark-transition terms. The partial widths for single-pion emission are given by²

$$\begin{aligned} \Gamma(A \rightarrow B\pi) &= \frac{1}{\pi f_\pi^2} \frac{p_\pi}{2J_A + 1} \frac{(M_A^2 - M_B^2)^2}{4M_A^2} \\ &\times \sum_\lambda |\langle A, \lambda | Q_5 | B, \lambda \rangle|^2, \end{aligned} \quad (9)$$

while those for single-photon emission are given by

$$\Gamma(A \rightarrow \gamma B) = \frac{e^2}{\pi} \frac{p_\gamma^3}{2J_A + 1} \sum_{\lambda_\gamma=1} |\langle A, \lambda | D_+ | B, \lambda - 1 \rangle|^2. \quad (10)$$

Here p_π and p_γ are the magnitude of the pion and photon 3-momenta in the rest frame of A ; the pion decay constant f_π is 135 MeV.

To facilitate the presentation of tables and the application of vector dominance we redefine helicity amplitudes $A_\lambda^{(\pi)}$, $A_\lambda^{(\gamma)}$, and $A_\lambda^{(\gamma\gamma)}$ for single-pion, single-photon, and two-photon processes. In terms of these new amplitudes the partial widths are given by

$$\Gamma(A \rightarrow B\pi) = \frac{p_\pi^3}{8\pi} \frac{1}{2J_A + 1} \sum_\lambda |A_\lambda^{(\pi)}|^2, \quad (11)$$

$$\Gamma(A \rightarrow \gamma B) = \frac{p_\gamma^3}{8\pi} \frac{2}{2J_A + 1} \sum_{\lambda_\gamma=1} |A_\lambda^{(\gamma)}|^2, \quad (12)$$

$$\Gamma(A \rightarrow \gamma\gamma) = \frac{p_\gamma^3}{8\pi} \frac{1}{2} \frac{2}{2J_A + 1} \sum_{\lambda_\gamma=1} |A_\lambda^{(\gamma\gamma)}|^2. \quad (13)$$

If one defines the transition matrix \mathfrak{M}_{fi} by

$$S_{fi} = \delta_{fi} + i(2\pi)^4 \delta^4(P_i - P_f) \mathfrak{M}_{fi} \mathfrak{N}_{fi}, \quad (14)$$

$$\mathfrak{N}_{fi} \equiv \prod_{i,j} (2E_i)^{-1/2} (2E_f)^{-1/2}$$

and helicity amplitudes (for decays) by

$$\mathfrak{M}_{A \rightarrow 1+2}(p, \lambda_1, \lambda_2, \Omega, J_{Az}) \\ = \mathfrak{D}_{J_{Az}, \lambda}^{J_A^*}(\Omega) \mathfrak{M}_{A \rightarrow 1+2}(p, \lambda_1, \lambda_2), \quad (15)$$

where $\lambda \equiv \lambda_1 - \lambda_2$, then

$$\mathfrak{M}_{A \rightarrow 1+2}(p, \lambda_1, \lambda_2) = M_A p_{A\lambda} \quad (16)$$

for all three cases. Here $p = p_\pi$ or p_γ and $A_\lambda = A_\lambda^{(\pi)}$, $A_\lambda^{(\gamma)}$, or $A_\lambda^{(\gamma\gamma)}$. We also have

$$A_\lambda^{(\pi)} = \frac{2\sqrt{2}}{f_\pi} \langle A, \lambda | Q_5 | B, \lambda \rangle \frac{p_{m_\pi=0}}{p_\pi} \quad (17)$$

for single-pion emission, and

$$A_\lambda^{(\gamma)} = 2e \langle A, \lambda | D_+ | B, \lambda = 1 \rangle \quad (18)$$

for single-photon emission. In Eq. (17),

$$p_{m_\pi=0} = \frac{M_A^2 - M_B^2}{2M_A} \rightarrow p_\pi \text{ as } m_\pi \rightarrow 0. \quad (19)$$

For the cases that will be of interest here, $p_{m_\pi=0}/p_\pi \cong 1$ to within about 4%.

We shall apply vector dominance in the following way:

$$A_\lambda(A \rightarrow \gamma\pi) = \frac{e}{g_\rho} A_\lambda(A \rightarrow \rho^0\pi) + \frac{e}{g_\omega} A_\lambda(A \rightarrow \omega\pi) \\ + \frac{e}{g_\phi} A_\lambda(A \rightarrow \phi\pi) \\ = \frac{e}{g_\rho} [A_\lambda(A \rightarrow \rho^0\pi) + \frac{1}{3}A_\lambda(A \rightarrow \omega\pi) \\ + \frac{1}{3}\sqrt{2}A_\lambda(A \rightarrow \phi\pi)]. \quad (20)$$

We then compare the following matrix elements:

$$A_{\lambda=1}^{(\gamma)}(A_2^+ \rightarrow \gamma\pi^+) = \frac{e}{g_\rho} A_{\lambda=1}^{(\pi)}(A_2^+ \rightarrow \rho^0\pi^+), \quad (21)$$

$$A_{\lambda=1}^{(\gamma)}(A_1^+ \rightarrow \gamma\pi^+) = \frac{e}{g_\rho} A_{\lambda=1}^{(\pi)}(A_1^+ \rightarrow \rho^0\pi^+), \quad (22)$$

$$A_{\lambda=1}^{(\gamma)}(B \rightarrow \gamma\pi) = \frac{e}{g_\omega} A_{\lambda=1}^{(\pi)}(B \rightarrow \omega\pi). \quad (23)$$

These relations lead, respectively, to^{2,12}

$$A_2: \frac{\sqrt{3}}{8} D(1, 1) + \frac{\sqrt{6}}{12} D(1, 0) \\ = \frac{\sqrt{2}}{g_\rho f_\pi} \left(-\frac{\sqrt{3}}{8} a + \frac{\sqrt{6}}{12} b \right), \quad (24)$$

$$A_1: -\frac{\sqrt{3}}{8} D(1, 1) + \frac{\sqrt{6}}{12} D(1, 0) \\ = \frac{\sqrt{2}}{g_\rho f_\pi} \left(\frac{\sqrt{3}}{8} a + \frac{\sqrt{6}}{12} b \right), \quad (25)$$

$$B: \frac{\sqrt{6}}{24} D(0, 0) = \frac{\sqrt{2}}{3g_\rho f_\pi} \frac{\sqrt{3}}{6} b. \quad (26)$$

We then find

$$\begin{cases} D(0, 0) \\ D(1, 1) \\ D(1, 0) \end{cases} = \frac{\sqrt{2}}{g_\rho f_\pi} \begin{cases} \frac{2}{3}\sqrt{2}b \\ -a \\ b \end{cases}. \quad (27)$$

The two-photon couplings are obtained by applying vector dominance once again in the same way:

$$A_\lambda(A \rightarrow \gamma\gamma) = \frac{e}{g_\rho} [A_\lambda(A \rightarrow \gamma\rho^0) + \frac{1}{3}A_\lambda(A \rightarrow \gamma\omega) \\ + \frac{1}{3}\sqrt{2}A_\lambda(A \rightarrow \gamma\phi)]. \quad (28)$$

We have summarized this information in Table I.

The first section of Table I is the most general single-quark-transition description of pion emission by $L=1$ mesons.² The second section is *not* the most general description of photon emission, which would contain three parameters rather than

TABLE I. Helicity amplitudes A_λ for pion and photon emission.

Process	Helicity	Coefficient of		Scale factor
		a	b	
$A_2^+ \rightarrow \rho^0\pi^+$	$\lambda=1$	$-\frac{1}{8}\sqrt{3}$	$\frac{1}{12}\sqrt{6}$	
$A_1^+ \rightarrow \rho^0\pi^+$	$\lambda=0$	0	$\frac{1}{6}\sqrt{6}$	
	$\lambda=1$	$\frac{1}{8}\sqrt{3}$	$\frac{1}{12}\sqrt{6}$	
$B^+ \rightarrow \omega\pi^+$	$\lambda=0$	$\frac{1}{8}\sqrt{6}$	0	$\frac{2\sqrt{2}}{f_\pi}$
	$\lambda=1$	0	$\frac{1}{6}\sqrt{3}$	
$f_0 \rightarrow \pi^+\pi^{-a}$	$\lambda=0$	$-\frac{1}{4}$	$\frac{1}{6}\sqrt{2}$	
$\epsilon \rightarrow \pi^+\pi^{-a}$	$\lambda=0$	$\frac{1}{8}\sqrt{2}$	$\frac{1}{3}$	
$A_2^+ \rightarrow \gamma\pi^+$	$\lambda=1$	$-\frac{1}{8}\sqrt{3}$	$\frac{1}{12}\sqrt{6}$	
$A_1^+ \rightarrow \gamma\pi^+$	$\lambda=1$	$\frac{1}{8}\sqrt{3}$	$\frac{1}{12}\sqrt{6}$	
$B \rightarrow \gamma\pi^+$	$\lambda=1$	0	$\frac{1}{18}\sqrt{3}$	
$\epsilon \rightarrow \gamma\rho^a$	$\lambda=0$	$-\frac{1}{8}\sqrt{2}$	0	$\frac{e}{g_\rho} \frac{2\sqrt{2}}{f_\pi}$
$D \rightarrow \gamma\rho^a$	$\lambda=0$	0	0	
	$\lambda=1$	$-\frac{1}{8}\sqrt{3}$	$\frac{1}{12}\sqrt{6}$	
$f_0 \rightarrow \gamma\rho^a$	$\lambda=0$	$\frac{1}{4}$	0	
	$\lambda=1$	$\frac{1}{8}\sqrt{3}$	$\frac{1}{12}\sqrt{6}$	
	$\lambda=2$	0	$\frac{1}{3}\sqrt{3}$	
$\epsilon \rightarrow \gamma\gamma^a$	$\lambda=0$	$-\frac{5}{36}\sqrt{2}$	0	
$D \rightarrow \gamma\gamma^a$	$\lambda=0$	0	0	$\left(\frac{e}{g_\rho}\right)^2 \frac{2\sqrt{2}}{f_\pi}$
$f_0 \rightarrow \gamma\gamma^a$	$\lambda=0$	$\frac{5}{18}$	0	
	$\lambda=2$	0	$\frac{10}{27}\sqrt{3}$	

^a f_0, D, ϵ taken as "ideally mixed" states involving non-strange quarks.

two.² However, Eq. (27) implies one constraint among these three parameters. It is precisely this constraint which leads to the vanishing of the $\lambda=0$ amplitude for $D \rightarrow \gamma \rho$. This amplitude is

$$A_{\lambda=0}(D \rightarrow \gamma \rho) \propto D(0, 0) - \frac{2}{3} \sqrt{2} D(1, 0) \quad (29)$$

in the more general description. Its vanishing is necessary, in fact, for the consistency of the vector-dominance hypothesis⁵: If we pass from $q^2=0$ to $q^2=m_\rho^2$ for the emitted photon, the residue of the ρ pole describes the emission of two identical transversely polarized spin-1 particles by a spin-1 particle. Yang has shown this cannot occur,¹³ so $A_{\lambda=0}(D \rightarrow \gamma \rho)$ must vanish, and

$$D(0, 0) = \frac{2}{3} \sqrt{2} D(1, 0). \quad (30)$$

Equation (27) implies an *overall scale* for photonic transitions in addition to the constraint implied by Eq. (30). Hence the predictions of Table I really test two *separate* pieces of physics over and above the single-quark-transition hypothesis: the constraint (30), and the overall scale (27) relating one-photon emission rates to those for one-pion emission. The tests of the latter might fail while the constraint (30) continued to hold. This would be reflected in relative agreement of predictions within a single section of Table I, but not of predictions relating one section to another.

III. NUMERICAL PREDICTIONS OF PARTIAL WIDTHS

In order to make use of Table I, one must estimate the reduced matrix elements a and b from known processes such as $A_2 \rightarrow \rho \pi$, $f_0 \rightarrow \pi \pi$, and $B \rightarrow \omega \pi$.

In the pionic decays considered here, there are two independent combinations of a and b , governing D -wave and S -wave decays, respectively;

$$D \equiv a - \frac{2}{3} \sqrt{2} b, \quad (31)$$

$$S \equiv a + \frac{4}{3} \sqrt{2} b. \quad (32)$$

The D -wave combination is known very precisely from processes such as $A_2 \rightarrow \rho \pi$, $f_0 \rightarrow \pi \pi$, and $SU(3)$ -related decays.¹⁴

The S -wave combination (32) may be estimated either from decays which are purely S -wave, e.g., $\delta \rightarrow \eta \pi$, or from decays which are largely so, e.g., $B \rightarrow \omega \pi$. This latter method was adopted in Ref. 14. The result was

$$\frac{a}{b} \cong \frac{1}{4}. \quad (33)$$

This value is consistent with the observed S -wave decay widths,¹⁴ though a slightly smaller value would be favored by $\delta \rightarrow \eta \pi$.

An independent estimate of a/b may be made

with the help of analyses of the spin parity of the B such as those performed in Ref. 15. There, it was found that

$$\frac{\Gamma_{\lambda=0}(B \rightarrow \omega \pi)}{\sum_{\lambda=\pm 1} \Gamma_{\lambda}(B \rightarrow \omega \pi)} = \begin{cases} 0.18 \pm 0.08 & \text{(Ref. 15a)} \\ 0.09 \pm 0.09 & \text{(Ref. 15b)} \end{cases} \quad (34)$$

which translates into

$$\left| \frac{a}{b} \right| = \begin{cases} 0.57 \pm 0.13 & \text{(Ref. 15a)} \\ 0.38 \pm 0.19 & \text{(Ref. 15b)} \end{cases} \quad (35)$$

with the help of Table I.

A third estimate, made primarily for simplicity in the first of Ref. 2, simply sets

$$\frac{a}{b} = 0. \quad (36)$$

This corresponds to a selection rule in which the $q\bar{q}$, $L=1$ meson always decays to $\pi + (q\bar{q}$, $L=0$ meson) with a change of one unit of L_z relative to the decay axis.

In view of the range of values just quoted for a/b , we shall present our results for the three values $a/b=0, \frac{1}{4}, \frac{1}{2}$. As mentioned, the combination $a - (2\sqrt{2}b/3)$ is fixed by the strength of D -wave decays. We shall take the best known of these, $\Gamma(A_2 \rightarrow \rho \pi) = 72$ MeV, as input.¹⁴

In order to apply the vector-dominance hypothesis, one needs a value of g_ρ . We have estimated this number in several ways. The leptonic width of the ρ meson is given by

$$\Gamma(\rho \rightarrow e^+ e^-) = \frac{m_\rho}{3} \frac{\alpha^2}{g_\rho^2 / 4\pi}. \quad (37)$$

If we use¹⁶ $\Gamma(\rho \rightarrow e^+ e^-) = 6.1 \pm 0.7$ keV, we obtain

$$\frac{g_\rho^2}{4\pi} = 2.2 \pm 0.3. \quad (38)$$

Here and elsewhere we take $m_\rho = 770$ MeV. The $\pi\pi$ width of the meson is given by

$$\Gamma(\rho \rightarrow \pi \pi) = \frac{2}{3} \frac{g_\rho^2}{4\pi} \frac{p^{*3}}{m_\rho^2}, \quad (39)$$

where $p^* = 359$ MeV/ c is the magnitude of the pion c.m.-system three momentum. If we use¹⁷ $\Gamma(\rho \rightarrow \pi \pi) = 150 \pm 10$ MeV, we find

$$\frac{g_\rho^2}{4\pi} = 2.9 \pm 0.2. \quad (40)$$

Finally, vector dominance relates such processes as $\omega \rightarrow \pi^0 \gamma$ and $\pi^0 \rightarrow \gamma \gamma$:

$$\Gamma(\pi^0 \rightarrow \gamma \gamma) = \frac{2}{3} \frac{\alpha}{g_\rho^2 / 4\pi} \left[\frac{p^*(\pi^0 \rightarrow \gamma \gamma)}{p^*(\omega \rightarrow \pi^0 \gamma)} \right]^3 \Gamma(\omega \rightarrow \pi^0 \gamma). \quad (41)$$

The values $\Gamma(\pi^0 \rightarrow \gamma \gamma) = 7.92 \pm 0.42$ eV (Ref. 18) and $\Gamma(\omega \rightarrow \pi^0 \gamma) = 870 \pm 50$ keV (Ref. 17) imply

$$\frac{g_\rho^2}{4\pi} = 3.0 \pm 0.2. \quad (42)$$

For the purposes of this calculation, we shall take a value consistent with (38), (41), and (42), namely

$$\frac{g_\rho^2}{4\pi} = 2.7. \quad (43)$$

There may be some real variation between the ρ mass-shell value (38) and the value at $q^2 = 0$ obtained from (42). The discrepancy between (38) and (42) given an idea of how well we expect vector dominance to work.

With the choices of parameters discussed above, the coefficients in Table I lead to the predictions of Table II.

Some interesting experiments to test the predictions of Table II will be discussed in the next section, but a few remarks are worth making at once.

(1) Values of a/b outside the range between 0 and $\frac{1}{2}$ are probably excluded by pionic decays. Within the constraints provided by the helicity structure of $B \rightarrow \omega\pi$ and the fixed value of D -wave widths, the S waves become too small if $a/b < 0$ and too large if $a/b > \frac{1}{2}$.

(2) The decay widths for $A_2^+ \rightarrow \gamma\pi^+$ and processes related by $SU(3)$ are independent of a/b . The decay $A_2^+ \rightarrow \gamma\pi^+$ is tied to $A_2^+ \rightarrow \rho^0\pi^+$ by vector dominance. We have used the latter process as an input, as mentioned above.

(3) Certain decay widths, e.g., that for $A_1^+ \rightarrow \gamma\pi^+$, are very sensitive to a/b . They involve con-

TABLE II. Partial widths and helicity-amplitude ratios for decays of positive-parity mesons.

Process	Quantity	$a/b = 0$	$a/b = 0.25$	$a/b = 0.5$	Experimental value
$A_2 \rightarrow \rho\pi$	Γ (MeV)	72 ^a	72 ^a	72 ^a	72 ^a
$f_0 \rightarrow \pi\pi^b$	Γ (MeV)	116	116	116	146 ± 16 ^c
$A_1(1100) \rightarrow \rho\pi$	Γ (MeV)	94	210	620	~300 ^d
	$A_0^{(\pi)}/A_1^{(\pi)}$	2	1.58	1.31	1 ^{c,d}
$B \rightarrow \omega\pi$	Γ (MeV)	75	144	390	125 ± 10 ^e
	$A_0^{(\pi)}/A_1^{(\pi)}$	0	0.27	0.53	{ 0.61 ± 0.14 } ^f { 0.40 ± 0.20 }
$\delta \rightarrow \eta\pi$	Γ (MeV)	37	88	270	50 ± 20
$\epsilon(1200) \rightarrow \pi\pi$	Γ (MeV)	940	2240	> 2 m_E	~600
$K_N(1250) \rightarrow K\pi$	Γ (MeV)	340	810	> 2 m_{K_N}	~450
$A_2^+ \rightarrow \gamma\pi^+$	Γ (keV)	348 ^g	348 ^g	348 ^g	
$K^{*+} \rightarrow \gamma K^+$	Γ (keV)	312	312	312	
$K^{*0} \rightarrow \gamma K^0$	Γ (keV)	0	0	0	
$A_1^+ \rightarrow \gamma\pi^+$	Γ (keV)	338	1000	3600	
$Q_A^+(1300) \rightarrow \gamma K^+$	Γ (keV)	376	1090	3900	
$Q_A^0(1300) \rightarrow \gamma K^0$	Γ (keV)	0	0	0	
$B^+ \rightarrow \gamma\pi^+$	Γ (keV)	108	200	490	
$Q_B^+(1300) \rightarrow \gamma K^+$	Γ (keV)	82	150	370	
$Q_B^0(1300) \rightarrow \gamma K^0$	Γ (keV)	327	605	1480	
$f_0 \rightarrow \gamma\rho$	Γ (keV)	750	1490	4000	
	$A_0^{(\gamma)}/A_1^{(\gamma)}$	0	0.11	0.22	
	$A_1^{(\gamma)}/A_2^{(\gamma)}$	0.35	0.45	0.54	
$f' \rightarrow \gamma\phi$	Γ (keV)	360	730	1960	
$D(1286) \rightarrow \gamma\rho$	Γ (keV)	150	150	150	
	$A_0^{(\gamma)}/A_1^{(\gamma)}$	0	0	0	
$f_0 \rightarrow \gamma\gamma$	Γ (keV)	4.3	8.0	20	
	$A_0^{(\gamma\gamma)}/A_2^{(\gamma\gamma)}$	0	0.11	0.22	
$A_2 \rightarrow \gamma\gamma$	Γ (keV)	1.7	3.2	8.0	
$f' \rightarrow \gamma\gamma$	Γ (keV)	0.59	1.1	2.8	
$\epsilon \rightarrow \gamma\gamma$	Γ (keV)	0	0.04	0.38	
$\delta \rightarrow \gamma\gamma$	Γ (keV)	0	0.04	0.37	

^a Input.

^b Other D -wave predictions are quoted in Ref. 14. These are independent of a/b .

^c Experimental values are from Ref. 17 unless noted otherwise.

^d Resonant behavior not established. Appears to be dominantly S -wave in $\rho\pi$ channel.

^e Total width. Other decay modes not established but 4π , $\delta\pi$ possible.

^f Refs. 15a, 15b, respectively.

^g Related by vector dominance to $A_2 \rightarrow \rho\pi$, which was used as an input, and hence independent of a/b .

structive interference between a and b , whereas we have fixed a quantity, Eq. (31), which involves destructive interference.

(4) *The decay widths for $K^*(\mathbb{C}=+)-\gamma K^0$ vanish.* This is a consequence of SU(3) invariance. It says that the neutral K^* resonances with $J^{PC}=1^{++}$ and 2^{++} cannot be excited in the Coulomb field of a nucleus. As a result, if one studies $K^0+(Z)\rightarrow Q^0+(Z)\rightarrow(K\pi\pi)^0+(Z)$, only the Q_B will contribute.

(5) *The decay widths for $f_0\rightarrow\gamma\rho$ and $f'\rightarrow\gamma\phi$ are quite large.* As an example, for $a/b=\frac{1}{4}$,

$$\frac{\Gamma(f_0\rightarrow\gamma\rho)}{\Gamma(f_0\rightarrow\text{all})} \cong 1\%, \quad (44)$$

$$\frac{\Gamma(f'\rightarrow\gamma\phi)}{\Gamma(f'\rightarrow\text{all})} \cong 1-2\%. \quad (45)$$

This suggests that one look for the processes $f_0\rightarrow\gamma\pi^+\pi^-$ and $f'\rightarrow\gamma K^+K^-$. These processes will have characteristic angular distributions sensitive to a/b , as will be discussed in Sec. IV.

(6) *The decay width for $f_0\rightarrow\gamma\gamma$ is appreciable.* For the favored value $a/b\cong\frac{1}{4}$, we find

$$\Gamma(f_0\rightarrow\gamma\gamma)\cong 8 \text{ keV}. \quad (46)$$

One would find a much smaller value if one took $b=0$ as in Ref. 19, but we cannot do this in our approach as the ratio of a/b is constrained by the helicity structure in $B\rightarrow\omega\pi$.²⁰

(7) *The dominant helicity amplitudes are $\lambda=\pm 2$ in $f_0\rightarrow\gamma\rho$ and $f_0\rightarrow\gamma\gamma$.* This conclusion holds as well for all SU(3)-related processes, e.g., $f'\rightarrow\gamma\phi$, $A_2\rightarrow\gamma\gamma$, $f'\rightarrow\gamma\gamma$. Table I implies

$$\begin{aligned} \frac{A_{\lambda=0}(f_0\rightarrow\gamma\rho)}{A_{\lambda=2}(f_0\rightarrow\gamma\rho)} &= \frac{A_{\lambda=0}(f_0\rightarrow\gamma\gamma)}{A_{\lambda=2}(f_0\rightarrow\gamma\gamma)} \\ &= \frac{1}{\sqrt{6}} \frac{A_{\lambda=0}(B\rightarrow\omega\pi)}{A_{\lambda=1}(B\rightarrow\omega\pi)}, \end{aligned} \quad (47)$$

and the right-hand side of Eq. (47) is known to be small experimentally.¹⁵ Equation (47) was first used in Ref. 21 to evaluate the helicity structure in $f_0\rightarrow\gamma\gamma$, but the assumptions used there were more restrictive.^{22,23}

(8) *The widths for $0^{++}\rightarrow\gamma\gamma$ are tiny.* They vanish altogether for $a=0$. The fact that b contributes neither to $0^{++}\rightarrow\gamma\gamma$ nor to the $\lambda=0$ amplitude for $2^{++}\rightarrow\gamma\gamma$ can be traced back to the constraint (30), which in turn follows from Yang's theorem¹³ as applied to $D\rightarrow\gamma\rho$. If a large signal is seen in $\gamma\gamma\rightarrow 0^{++}\rightarrow\pi^+\pi^-$, we would expect it to be due to something other than a $q\bar{q}$ state, for example a dilaton.²⁴ A dilaton could *not* explain $\gamma\gamma\rightarrow\delta(0^{++})$ since δ has $I=1$; we expect this process to be greatly suppressed. For $a/b=\frac{1}{4}$, we expect

$$\Gamma(\delta^0\rightarrow\gamma\gamma)\cong 40 \text{ eV}. \quad (48)$$

In contrast, Sec. IV contains a prediction:

$$\Gamma(\eta'\rightarrow\gamma\gamma)=6.4 \text{ keV}. \quad (49)$$

(The η' is very close in mass to the δ^0 ; $\eta'\rightarrow\gamma\pi^+\pi^-$ and $\eta'\rightarrow\eta\pi\pi$ are its dominant decay modes, to be contrasted with $\delta^0\rightarrow\eta\pi^0$.) Hence, in a $\gamma\gamma$ experiment sensitive to η' we would expect the production of the δ^0 to be less than 10^{-2} that of the η' .

IV. CROSS SECTIONS AND ANGULAR DISTRIBUTIONS

In this section we develop further experimental consequences of our predictions. These relate to three major areas: cross sections for Primakoff effect, cross sections for two-photon processes, and angular distributions.

A. Cross sections for Primakoff effect

The Coulomb dissociation of pions²⁵ and kaons²⁶ in the field of a nucleus already has been studied at Brookhaven. Even at these energies, it has been shown that one can detect partial widths of less than 100 keV when the excited particles are relatively light. Similar experiments at Fermilab⁸ will be able to extend the mass range of the excited particles to nearly 2 GeV.

The first processes likely to be measurable at Fermilab are those that have been measured at lower energies. It has been noted^{25,26} that the measured rates for $\rho^-\rightarrow\pi^-\gamma$ and $K^{*0}\rightarrow K^0\gamma$ are about a factor of 3 lower than one would expect from SU(3) invariance and the measured rate¹⁷ for $\omega\rightarrow\pi^0\gamma$. The single-quark-transition and VDM hypotheses also lead to predictions of rates considerably larger than those measured and in accord with those predicted by SU(3) alone. For example, if one neglects the pion mass, one finds

$$\Gamma(\rho^-\rightarrow\pi^-\gamma) = \frac{2}{9} \frac{\alpha}{g_\rho^2/4\pi} \Gamma(\rho\rightarrow\pi\pi) \quad (50)$$

$$= 90 \text{ keV}. \quad (51)$$

SU(3) predicts

$$\Gamma(\rho^-\rightarrow\pi^-\gamma) = \frac{1}{9} \Gamma(\omega\rightarrow\pi^0\gamma) \quad (52)$$

$$= 97 \pm 6 \text{ keV} \quad (53)$$

(if we take $m_\rho=m_\omega$), while the number quoted in Ref. 25 is 35 ± 10 keV. Similarly one may relate $K^*\rightarrow K\gamma$ to $\rho^-\rightarrow\pi^-\gamma$ with the help of SU(3). If one starts from Eq. (51) the results are the predictions

$$\Gamma(K^{*-}\rightarrow K^-\gamma) = 50 \text{ keV}, \quad (54)$$

$$\Gamma(K^{*0}\rightarrow K^0\gamma) = 200 \text{ keV}. \quad (55)$$

The latter figure is to be compared with the experimental value²⁶ $\Gamma(K^{*0}\rightarrow K^0\gamma) = 75 \pm 35$ keV. Clearly the resolution of these discrepancies will be the first order of business in Coulomb dis-

sociation experiments at high energies. (Our approach seems to be somewhat less flexible than that of Ref. 27)

The π^0 and η have been studied via the Primakoff effect²⁸ at lower energies. One new (relatively light) meson that one could expect to study at higher energies is the η' , whose predicted $\gamma\gamma$ width (on the basis of the single-quark-transition hypothesis) is

$$\begin{aligned} \Gamma(\eta' \rightarrow \gamma\gamma) &= \left(\frac{m_{\eta'}}{m_{\pi^0}}\right)^3 \left[2\left(\frac{2}{3}\right)^{1/2} \cos\theta - \frac{1}{\sqrt{3}} \sin\theta \right]^2 \\ &\times \Gamma(\pi^0 \rightarrow \gamma\gamma) \\ &= 6.4 \text{ keV}, \end{aligned} \quad (56)$$

as noted in Eq. (49). Here θ is the octet-singlet mixing angle,²⁹ chosen to be 10.4° , and $\Gamma(\pi^0 \rightarrow \gamma\gamma)$ is taken from Ref. 18. The measurement of $\Gamma(\eta' \rightarrow \gamma\gamma)$ would allow the evaluation of $\Gamma(\eta' \rightarrow \rho\gamma)$, $\Gamma(\eta' \rightarrow \eta\pi\pi)$, and $\Gamma_{\text{tot}}(\eta')$ as well, since the branching ratios for all these modes are fairly well known. Indeed, the ratio $\Gamma(\eta' \rightarrow \gamma\gamma)/\Gamma(\eta' \rightarrow \rho\gamma)$ is another test of the vector-dominance hypothesis which seems to be passed satisfactorily.^{27,30,31}

The corresponding prediction for $\eta \rightarrow \gamma\gamma$ is

$$\begin{aligned} \Gamma(\eta \rightarrow \gamma\gamma) &= \left(\frac{m_{\eta}}{m_{\pi^0}}\right)^3 \left[\frac{\cos\theta}{\sqrt{3}} + 2\left(\frac{2}{3}\right)^{1/2} \sin\theta \right]^2 \\ &\times \Gamma(\pi^0 \rightarrow \gamma\gamma) \\ &= 396 \pm 21 \text{ eV}, \end{aligned} \quad (57)$$

to be compared with the present experimental value³²

$$\Gamma(\eta \rightarrow \gamma\gamma) = 324 \pm 46 \text{ eV}. \quad (58)$$

When one comes to the positive-parity mesons, the predicted $\pi\gamma$, $K\gamma$, and $\gamma\gamma$ widths of Table II are very encouraging for Primakoff-effect studies. The cross section for the Primakoff effect is⁷

$$\frac{d\sigma}{d\Omega} \Big|_{B \rightarrow A} = Z^2 \alpha |F(q^2)|^2 \frac{\Gamma(A \rightarrow B\gamma)}{p_\gamma^{*3}} \frac{\theta^2}{(\theta^2 + \delta^2)^2} X_{AB}. \quad (59)$$

Here Z is the charge of the nucleus, $F(q^2)$ is its form factor, S_A is the spin of particle A , θ is the laboratory scattering angle,

$$p_\gamma^* = \frac{M_A^2 - M_B^2}{2M_A} \quad (60)$$

is the c.m. three-momentum of the photon in the decay $A \rightarrow B\gamma$,

$$\delta \equiv \frac{M_A^2 - M_B^2}{2E^2}, \quad (61)$$

where E is the beam energy,

$$q^2 = -E^2(\theta^2 + \delta^2) \equiv -Q^2 \quad (62)$$

is the invariant momentum transfer, and

$$\begin{aligned} X_{AB} &= \frac{\eta'_B}{\eta_B} \frac{2S_A + 1}{2S_B + 1}, \\ \eta_B &= \begin{cases} 1, & B \neq \gamma \\ \frac{1}{2}, & B = \gamma \end{cases} \\ \eta'_B &= \begin{cases} 1, & m_B \neq 0 \\ \frac{1}{2}(2S_B + 1), & m_B = 0 \end{cases} \end{aligned} \quad (63)$$

is a statistical factor. The nuclear form factors have been parametrized according to³³

$$F(q^2) = \exp\left(-\frac{1}{6} Q^2 \langle R^2 \rangle\right), \quad (64)$$

and Eq. (59) integrated to obtain the cross sections shown in Table III. In addition to Eqs. (49), (51), (54), (55), (57), and the partial widths quoted in Table II, we have made use of the single-quark-transition³⁴ and vector-dominance-model result

$$\begin{aligned} \Gamma(g^- \rightarrow \pi^- \gamma) &= \frac{4}{27} \frac{\alpha}{g_\rho^2/4\pi} \Gamma(g \rightarrow \pi\pi) \\ &\simeq (4 \times 10^{-4})(40 \text{ MeV}) \\ &= 16 \text{ keV}. \end{aligned} \quad (65)$$

The g is a spin-3 isovector meson at 1680 MeV,¹⁷ the Regge recurrence of the ρ . The pion mass has been neglected in deriving (65).

Table III shows that many processes involving excitation of the higher-mass mesons should be as easy to study as ρ , K^* , π^0 , and η excitation, which already have been seen at lower energies. For example, we note the following

(1) *Coulomb excitation of the A_1^\pm and Q_A^\pm should be considerable.* Diffractive hadronic excitation of these resonances (due to the Pomeron) also will occur. It may be possible to separate the two processes from one another on the basis of different helicity structures; if excitation occurs in the *same* helicity amplitudes it may be possible to separate the Coulomb and hadronic contributions by using beams of both signs.

(2) *The A_2^\pm and $K^{*+}(1420)$ should be prominent.* This was anticipated in Ref. 8; our estimates are somewhat less optimistic than theirs, however. These estimates are insensitive to the value of a/b , in contrast to the estimates for A_1^\pm and Q_A^\pm production.

(3) *The Q_B^0 signal should be detectable.* It is fairly sensitive to a/b . There will be a background of diffractive *hadronic* excitation of Q_A^0 , however. The most promising final state for study of this system would be $K_S^0 \pi^+ \pi^-$. If Coulomb-Pomeron interference occurs, the π^+ and π^- in this final state need not be symmetric in their momenta and angular distributions.

(4) *The π^0 , η' , and f_0 signals all should be comparable to one another for incident 100-GeV pho-*

TABLE III. Expected cross sections for Coulomb excitation of resonances.

Beam A (energy)	Excited state B	Assumed $\Gamma(B \rightarrow A\gamma)$	σ (μb) on		
			C $\langle R^2 \rangle^{1/2} = 2.37 \text{ fm}$	Cu $\langle R^2 \rangle^{1/2} = 4.03 \text{ fm}$	Pb $\langle R^2 \rangle^{1/2} = 5.42 \text{ fm}$
π^- (200 GeV)	$\rho^-(770)$	90 keV ^a	13	260	1900
	$A_1^-(1100)$	1 MeV ^b	38	730	5200
	$B^-(1237)$	200 keV	5	93	650
	$A_2^-(1310)$	350 keV	11	210	1500
	$g^-(1680)$	16 keV ^c	0.3	5	33
K^- (200 GeV)	$K^{*-}(890)$	50 keV ^d	13	250	1800
	$Q_A^-(1300)$	1 MeV	33	620	4400
	$Q_B^-(1300)$	150 MeV	5	93	650
	$K^{*-}(1420)$	300 keV	11	200	1400
K^0 (100 GeV)	$K^{*0}(890)$	200 keV ^e	52	1000	7400
	$Q_B^0(1300)$	600 keV	20	370	2600
γ (100 GeV)	$\pi^0(135)$	7.92 eV ^f	0.10	2.1	16
	$\eta(549)$	396 eV ^g	0.05	0.93	6.8
	$\eta'(958)$	6.4 keV ^h	0.10	1.9	13
	$f_0(1270)$	8 keV	0.21	3.7	25

^a Based on Eq. (51).

^b Except as noted otherwise, assumed partial widths are rounded-off values based on Table II for $a/b = \frac{1}{4}$. Coulomb-excitation cross sections are directly proportional to partial widths and may be scaled accordingly. [See Eq. (59).]

^c Based on Eq. (65).

^d Based on Eq. (54).

^e Based on Eq. (55).

^f Ref. 18.

^g Based on Eq. (57).

^h Based on Eq. (56).

tons. The Primakoff excitation of f_0 is an interesting possibility. It may not be easy, since the f_0 is relatively broad, and other processes could contribute to the $\pi^+\pi^-$ final state. An alternative for detecting the large $f_0\gamma\gamma$ coupling is the use of colliding beams, which we describe below.

B. Cross sections for two-photon processes

For $m(\gamma\gamma)$ between 1 and 1.5 GeV the process $\gamma\gamma \rightarrow \pi^+\pi^-$ is expected to be dominated by the f_0 , and $\gamma\gamma \rightarrow K^+K^-$ should be dominated by the f_0 , A_2 , and f' .¹⁹ We can estimate rates for these processes on the basis of Table II. These rates are best compared with the rate of nonresonant muon production: $\gamma\gamma \rightarrow \mu^+\mu^-$, calculable from quantum electrodynamics. The cross section for this latter process is^{9,35}

$$\sigma_T(\gamma\gamma \rightarrow \mu^+\mu^-) \cong \frac{4\pi\alpha^2}{s} \left(\ln \frac{s}{m_\mu^2} - 1 \right). \quad (66)$$

Here s is the square of the total energy in the photon-photon center of mass. A high- s approximation has been used to obtain Eq. (66). When the geometric acceptance is a function of muon direction, a differential cross section must be

used in place of Eq. (66). This cross section is presented in the Appendix.

The total cross section for $\gamma\gamma \rightarrow \pi^+\pi^-$ in the region of the f_0 may be written as

$$\sigma_T(\gamma\gamma \rightarrow f_0 \rightarrow \pi^+\pi^-) = \frac{20\pi}{3s} \frac{\Gamma_{\pi\pi}\Gamma_{\gamma\gamma}}{(\sqrt{s} - m_f)^2 + \frac{1}{4}\Gamma_f^2}. \quad (67)$$

Correspondingly, the ratio of $\pi^+\pi^-$ production to $\mu^+\mu^-$ production is

$$\frac{\sigma_T(\gamma\gamma \rightarrow f_0 \rightarrow \pi^+\pi^-)}{\sigma_T(\gamma\gamma \rightarrow \mu^+\mu^-)} = \frac{5}{3\alpha^2} \frac{\Gamma_{\pi\pi}\Gamma_{\gamma\gamma}}{(\sqrt{s} - m_f)^2 + \frac{1}{4}\Gamma_f^2} \times \left(\ln \frac{s}{m_\mu^2} - 1 \right)^{-1}. \quad (68)$$

In Figure 1 we have plotted Eq. (68) as a function of \sqrt{s} for the different values of $\Gamma_{\gamma\gamma}$ quoted in Table II. We have used $\Gamma_{\pi\pi} = 141 \text{ MeV}$ and $\Gamma_f = 170 \text{ MeV}$. [Note added in proof. The most recent values for these quantities, quoted in Ref. 17, are $\Gamma_{\pi\pi} = 146 \text{ MeV}$ and $\Gamma_f = 180 \text{ MeV}$.] One sees that the total rates for pion production at $\sqrt{s} = m_f$ are comparable to those for muon production. However, the angular distributions are expected to be rather different. The muons tend to be peaked at 0° and 180° in the pho-

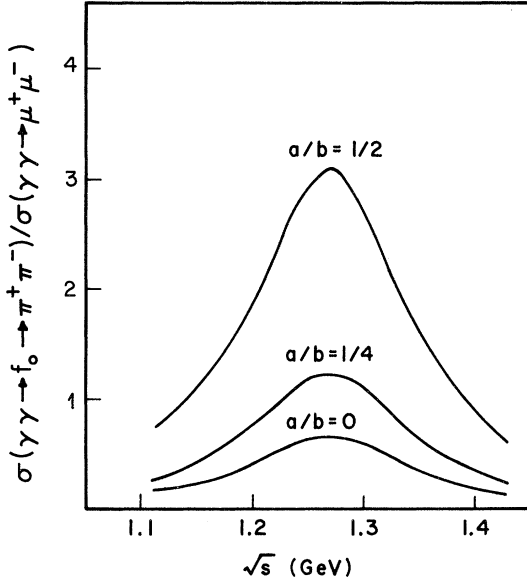


FIG. 1. Ratio of pion-pair production to muon-pair production in photon-photon reactions as a function of \sqrt{s} .

ton-photon center of mass³⁵ (see the Appendix). By contrast, we shall see in the next subsection that the pions are expected to be produced most copiously at 90° in this frame. With present geometries, this tends to enhance the probability of their detection.³⁶

C. Angular distributions

Consider first the process $\gamma\gamma \rightarrow f_0$. This can occur in states of total helicity ± 2 or 0 , with amplitudes $A_2 = A_{-2}$ and A_0 . Angular distributions of the decay products of the f_0 provide information on A_0/A_2 , which is predicted to be *small* in Table II. This will provide a crucial test of the marriage of the vector-dominance and single-quark-transition hypotheses.

In the processes

$$e^\pm e^- \rightarrow e^\pm e^- f_0 \quad (69)$$

$$\mathfrak{M}(\gamma\gamma \rightarrow f_0 \rightarrow \pi\pi) = f(E_{\text{c.m.}}) \sum_{\lambda_1, \lambda_2 = \pm 1} A_{\lambda_1 - \lambda_2} e^{i(\lambda_1 - \lambda_2)\phi} d_{\lambda_1 - \lambda_2, 0}^2(\theta) (\delta_{\lambda_1, -1} e^{i\psi} - \delta_{\lambda_1, 1} e^{-i\psi}) (\delta_{\lambda_2, 1} - \delta_{\lambda_2, -1}). \quad (71)$$

The last two terms in Eq. (71) describe the linearly polarized photons γ_1 and γ_2 . Performing the sum over helicities, one finds

$$|\mathfrak{M}(\gamma\gamma \rightarrow f_0 \rightarrow \pi\pi)|^2 = |f(E_{\text{c.m.}})|^2 \left[\frac{1}{2} \sqrt{6} A_2 \sin^2 \theta \cos(2\phi - \psi) - A_0 (3 \cos^2 \theta - 1) \cos \psi \right]^2. \quad (72)$$

Suppose that only one of the electrons in Eq. (69) were tagged. Then one would average over ψ in Eq. (72) to obtain

$$\langle |\mathfrak{M}(\gamma\gamma \rightarrow f_0 \rightarrow \pi\pi)|^2 \rangle_\psi = |f(E_{\text{c.m.}})|^2 \left[\frac{3}{4} A_2^2 \sin^4 \theta - \frac{1}{2} \sqrt{6} A_0 A_2 \sin^2 \theta (3 \cos^2 \theta - 1) \cos 2\phi + \frac{1}{2} A_0^2 (3 \cos^2 \theta - 1)^2 \right]. \quad (73)$$

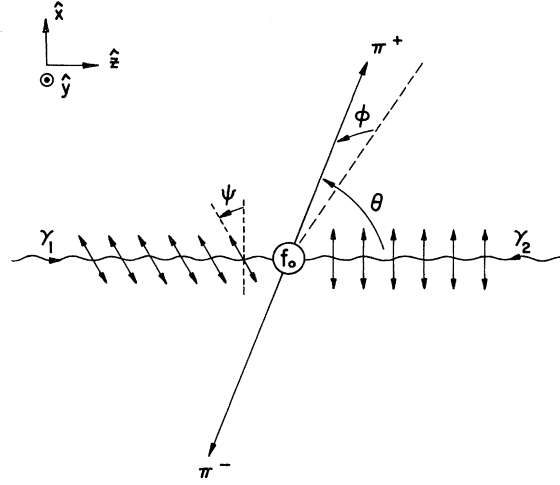


FIG. 2. Definition of angles for pion pair production by polarized photons. The angle between planes of photon polarization is ψ . The second photon is taken to be polarized in the x - z plane. The polar and azimuthal angles of the π^+ (in the c.m. system) are θ and ϕ .

and

$$\gamma Z \rightarrow f_0 Z \quad (70)$$

it is possible to study $\gamma\gamma \rightarrow f_0$ when both photons have linear polarizations making an arbitrary angle ψ with respect to one another in the center of mass. In process (69), ψ is the azimuthal angle between the two tagged final electrons. In process (70) it is necessary to polarize the incident photon; the exchanged photon is polarized linearly in the reaction plane. Information on ψ is useful but not necessary for our purposes.

The final pions emerge back to back in the center of mass; let the polar and azimuthal angles of the π^+ be (θ, ϕ) with respect to one of the incident photons (see Fig. 2). We have defined the x axis in Fig. 2 by the demand that the second photon γ_2 be polarized in the x - z plane.

It is then a simple exercise in kinematics to write the amplitude for $\gamma\gamma \rightarrow f_0 \rightarrow \pi\pi$ as a function of the two independent helicity amplitudes $A_2 = A_{-2}$ and A_0 :

This expression still contains azimuthal dependence unless A_0 or A_2 is zero. Finally, if neither electron is tagged, one averages Eq. (73) over ϕ and the middle term vanishes. Dominance of A_0 leads to a $\pi\pi$ distribution peaked at $\theta=0^\circ, 180^\circ$. This will be hard to detect in the process of Eq. (69), as the pions are then projected along the beam pipe. By contrast, dominance of A_2 leads to a $\pi\pi$ distribution peaked at $\theta=90^\circ$, the most favorable situation for observing the pion pair in either reaction (69) or reaction (70).^{9,10} In fact, we expect A_2 to be dominant. If $A_0=0$ Eq. (72) has an interesting property. When integrated over either ψ or ϕ , it is independent of the other variable of the pair. It has strong correlations in ψ and ϕ , however. Consequently an interesting quantity to plot (if it were available) would be $|\mathfrak{M}|^2$, for fixed $2\phi - \psi$, integrated over ψ . If $A_0=0$ this quantity should behave as $\cos^2(2\phi - \psi)$. In polar coordinates this resembles a four-leaf clover.

A convenient form for Eq. (72) may be obtained by defining

$$\rho \equiv \frac{-3\sqrt{2}}{4} \frac{a}{b}. \quad (74)$$

Then the single-quark-transition prediction is that

$$\begin{aligned} & |\mathfrak{M}(\gamma\gamma \rightarrow f_0 \rightarrow \pi\pi)|^2 \\ &= \text{const} \times [\sin^2\theta \cos(2\phi - \psi) + \rho(\cos^2\theta - \frac{1}{3})\cos\psi]^2, \end{aligned} \quad (75)$$

where ρ is constrained by the experimental numbers of Table II to lie somewhere between 0 and $\cong -\frac{1}{2}$.

The correlations between ψ and ϕ are potentially important in extracting $\Gamma(f_0 \rightarrow \gamma\gamma)$ from any experiment with limited acceptance. Similar correlations exist between ψ and ϕ for $\gamma\gamma \rightarrow \mu^+\mu^-$, a process which can serve as a "calibration" for $\gamma\gamma \rightarrow \pi^+\pi^-$.³⁵ Consequently, these correlations are discussed in the Appendix.

The predictions of helicity amplitude ratios for $f_0 \rightarrow \gamma\rho \rightarrow \gamma\pi^+\pi^-$ are easily tested. Consider the rest frame of the ρ , with the photon traveling along the positive z axis (see Fig. 3). Let the π^+ make an angle θ with the photon in this frame. Then the distribution in θ is

$$W(\theta) \propto (|A_2|^2 + |A_0|^2)^{\frac{1}{2}} \sin^2\theta + |A_1|^2 \cos^2\theta \quad (76)$$

or

$$W(\theta) \propto 1 + x \sin^2\theta, \quad (77)$$

with

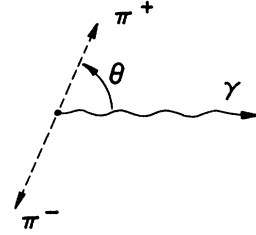


FIG. 3. Reference frame for discussions of $f_0 \rightarrow \gamma\rho \rightarrow \gamma\pi^+\pi^-$.

$$x = \begin{Bmatrix} 3 \\ 1.5 \\ 0.8 \end{Bmatrix} \text{ for } a/b = \begin{Bmatrix} 0 \\ \frac{1}{4} \\ \frac{1}{2} \end{Bmatrix}. \quad (78)$$

This distribution is relatively sensitive to a/b because of the constructive interference of a and b in the $\lambda=1$ amplitude. More generally, in terms of the parameter ρ of Eq. (74), we find the distribution

$$W(\theta) \propto 1 + \frac{3+2\rho - \frac{1}{3}\rho^2}{(1-\rho)^2} \sin^2\theta. \quad (79)$$

We remind the reader that Table II contains predictions of the relative phases of $A_0^{(\gamma)}$, $A_1^{(\gamma)}$, and $A_2^{(\gamma)}$. Even though Eq. (76) is not sensitive to these phases, one can imagine tests which can determine these phases. These would require the preparation of the f_0 in a definite state of polarization, as indeed is the case in most production reactions such as $\pi^-p \rightarrow f_0 n$ or $\pi^+p \rightarrow f_0 \Delta^{++}$.

V. SUMMARY AND CONCLUSIONS

The radiative decays of mesons with $J^{PC} = 2^{++}, 1^{++}, 0^{++}, 1^{+-}$ provide several useful tests of the notions of vector dominance and single quark transitions. We have presented rates and angular distributions based on these hypotheses, and have discussed the constraints that follow from demanding a consistent description of pion and photon emission.

The crucial experiments lie in the near future. They involve Coulomb excitation of hadrons, studies of two-photon processes in colliding lepton beams, and detection of particularly large radiative decay widths for processes such as $f_0 \rightarrow \gamma\rho$. In addition to testing the hypotheses mentioned above, such experiments can shed further light on the relative sizes of various reduced matrix elements in the theory. The ratios of these reduced matrix elements can point the way to further possible selection rules in the decays of orbitally excited hadrons. As an example, we have mentioned that the predominance of trans-

versely polarized ω 's in $B \rightarrow \omega\pi$ should reflect itself in a predominance of $\lambda = \pm 2$ in $f_0 \rightarrow \gamma\gamma$.

Other authors have come to similar conclusions about the helicity structure and partial width in $f_0 \rightarrow \gamma\gamma$ working from assumptions quite different from ours. Schrempp-Otto, Schrempp, and Walsh³⁷ saturated finite-energy sum rules for $\gamma\pi^0 \rightarrow \gamma\pi^0$ with the ω in the s channel and with the f_0 and ϵ in the t channel. They found

$$\Gamma(f \rightarrow \gamma\gamma) = 5.7 \text{ keV},$$

$$A_0^{(\gamma\gamma)}/A_2^{(\gamma\gamma)} \ll 1.$$

However, they also found

$$\Gamma(\epsilon \rightarrow \gamma\gamma) = 22.2 \text{ keV}.$$

This last relation is not necessarily in contradiction with our results, if the ϵ in their saturation scheme is not a $q\bar{q}$ state. If it is such a state, as the authors of Ref. 37 mention, the width $\Gamma(\delta \rightarrow \gamma\gamma)$ should be appreciable and the δ should be visible in colliding lepton-beam experiments. This would be in direct contradiction to our predictions.

Renner³⁸ obtained $\Gamma(f \rightarrow \gamma\gamma) = 8 \text{ keV}$ from an assumption of tensor-meson dominance of the Pomeron. A similar helicity structure to ours results, as a result of the crossing properties of helicity amplitudes. More recently, Grassberger and Kogerler³⁹ have obtained $A_0^{(\gamma\gamma)}/A_2^{(\gamma\gamma)} \ll 1$ in a slightly different treatment than that of Ref. 37.

These independent predictions of $A_0^{(\gamma\gamma)}/A_2^{(\gamma\gamma)}$ are very reassuring. They indicate that there may be fundamental reasons for the smallness of the ratio a/b .⁴⁰ This ratio is a free parameter in the single-quark-transition description, but it contains important dynamical information that can be used to test more specific models.

ACKNOWLEDGMENT

We are very grateful to Professor Earl A. Peterson for several illuminating discussions and for continual encouragement.

APPENDIX: ANGULAR DISTRIBUTIONS FOR $\gamma\gamma \rightarrow \mu^+\mu^-$

Experiments detecting $e^+e^- \rightarrow e^+e^-\pi^+\pi^-$ also will detect $e^+e^- \rightarrow e^+e^-\mu^+\mu^-$; in fact, the latter process probably will dominate the former (see Fig. 1). There are potentially errors of some tens of percent associated with the use of the "equivalent-photon approximation."³⁵ These can be avoided to a large extent simply by comparing rates for the two processes; these rates ought to scale in the ratio of the cross sections for $\gamma\gamma \rightarrow f_0 \rightarrow \pi^+\pi^-$ relative to $\gamma\gamma \rightarrow \mu^+\mu^-$.

When the final electrons are tagged, the plane in which they are scattered reflects the plane of polarization of the photons. Let E be the initial lepton energy, E' the final lepton energy, $\omega = E - E'$ the photon energy, and θ' the scattering angle of the lepton. Denote by I_\perp and I_\parallel the intensities of photons with polarizations perpendicular and parallel to the plane formed by the initial and final leptons. Then an approximate expression for the ratio of these intensities is

$$\frac{I_\perp}{I_\parallel} = \left(\frac{\omega}{2E - \omega} \right)^2. \quad (\text{A1})$$

This expression is valid when

$$\theta' \gg \frac{m_e(E - E')}{EE'} \quad (\text{A2})$$

and

$$\omega^2 \gg EE'\theta'^2, \quad (\text{A3})$$

both of which conditions hold for the geometry to be used at SPEAR.¹⁰ [Equation (A2) is not in contradiction with the equivalent-photon limit, which requires only that $\theta' \lesssim (m_e/E)^{1/2}$. On the other hand, this last bound is not satisfied by the present SPEAR experiment, and hence corrections to the equivalent-photon limit will be important. These corrections should largely cancel one another when one compares $\gamma\gamma \rightarrow \pi\pi$ and $\gamma\gamma \rightarrow \mu\mu$.]

When ω is small, the photons are predominantly linearly polarized in the plane of the tagged electron. As ω approaches the full beam energy, the ratio (A1) approaches unity and the photons become unpolarized.

When low-mass $\pi\pi$ or $\mu\mu$ pairs are produced via the reactions $e^+e^- \rightarrow e^+e^- + (\pi^+\pi^- \text{ or } \mu^+\mu^-)$, the square of the center-of-mass energy s is related to the photon energies by

$$s = 4\omega\omega'. \quad (\text{A4})$$

Consequently, one photon must have energy less than $\frac{1}{2}\sqrt{s}$, and hence will have a high degree of linear polarization if $\sqrt{s} \ll 2E$. When the $\pi\pi$ or $\mu\mu$ system is approximately at rest in the c.m. of the initial electron and positron, *both* photons will have a high degree of linear polarization. This can be important if the geometrical acceptance is limited in azimuthal

Because of these potential polarization effects, we have quoted cross sections in the text for $\gamma\gamma \rightarrow f_0 \rightarrow \pi^+\pi^-$ for photons with arbitrary linear polarizations with respect to one another (see Fig. 2). A similar expression can be written for $\gamma\gamma \rightarrow \mu^+\mu^-$. The result is ($z \equiv \cos\theta$):

$$\frac{d\sigma}{d\Omega}(\gamma\gamma \rightarrow \mu^+ \mu^-) = \frac{2\alpha^2\beta}{s}(1 - \beta^2 z^2)^{-1}[\sin^2\psi + \beta^2 z^2 \cos^2\psi + \beta^2(1 - z^2)\sin 2(\phi - \psi)\sin 2\phi + 4(1 - \beta^2 z^2)^{-1}\beta^2(1 - z^2)(1 - \beta^2)\cos^2(\phi - \psi)\cos^2\phi]. \quad (\text{A5})$$

Here the angles ψ , ϕ , and θ are as defined in Fig. 2, while $\beta \equiv (1 - 4m_\mu^2/s)^{1/2}$ is the velocity of each muon in the photon-photon center of mass. When averaged over ψ and integrated over ϕ and θ , Eq. (A5) gives the expression (66) used in the text. As in the case of $\gamma\gamma \rightarrow \pi^+\pi^-$, Eq. (A5) displays strong correlations in ϕ and ψ .

*Work supported in part by the Energy Research and Development Administration under Contract No. AT(11-1)-1764.

¹H. J. Melosh IV, Phys. Rev. D **9**, 1095 (1974); thesis, California Institute of Technology, 1973 (unpublished).

²F. Gilman, M. Kugler, and S. Meshkov, Phys. Rev. D **9**, 715 (1974); pion emission by mesons and baryons; A. J. G. Hey, J. Rosner, and J. Weyers, Nucl. Phys. B**61**, 205 (1973); pion emission by mesons; F. Gilman and I. Karliner, Phys. Rev. D **10**, 2194 (1974) and A. J. G. Hey and J. Weyers, Phys. Lett. **48B**, 69 (1974): photon emission.

³A. J. G. Hey, P. J. Litchfield, and R. J. Cashmore, Nucl. Phys. B**95**, 516 (1975); R. J. Cashmore, A. J. G. Hey, and P. J. Litchfield, *ibid.* B**98**, 237 (1975): pion and photon emission by baryons.

⁴J. Babcock and J. Rosner, Ann. Phys. (N.Y.) **96**, 191 (1976): photon emission by baryons.

⁵J. Babcock and J. Rosner, Phys. Rev. D **12**, 2761 (1975).

⁶G. Karl, S. Meshkov, and J. Rosner, Phys. Rev. D **13**, 1203 (1976).

⁷A. Halprin, C. M. Andersen, and H. Primakoff, Phys. Rev. **152**, 1295 (1966).

⁸T. Ferbel (spokesman), Fermilab approved experiment E-272, 1975 (unpublished).

⁹For a review of the extensive literature see H. Terazawa, Rev. Mod. Phys. **45**, 615 (1973).

¹⁰One of us (J.R.) thanks G. Masek for an informative discussion regarding this experiment.

¹¹The fact that such constraints might exist was mentioned in the first of Refs. 2; the explicit form of these constraints was given in Ref. 4 and further discussions may be found in Refs. 5 and 6.

¹²Note that with respect to the pionic-decay tables of Gilman, Kugler, and Meshkov, Ref. 2, we use the SU(6) Clebsch-Gordan coefficients of C. L. Cook and G. Murtaza, Nuovo Cimento **39**, 531 (1965), and we flip the order of final states.

¹³C. N. Yang, Phys. Rev. **77**, 242 (1950).

¹⁴J. Rosner, Phys. Reports **11C**, 189 (1974).

¹⁵(a) S. U. Chung *et al.*, Phys. Rev. D **11**, 2426 (1975); (b) U. Karshon *et al.*, *ibid.* **10**, 3608 (1974).

¹⁶D. Benaksas *et al.*, Phys. Lett. **39B**, 289 (1972). These authors quote $g_\rho^2/4\pi = 2.26 \pm 0.25$, taking $m_\rho = 775$ MeV.

¹⁷Particle Data Group, Rev. Mod. Phys. **48**, S1 (1976).

¹⁸A. Browman *et al.*, Phys. Rev. Lett. **33**, 1400 (1974).

¹⁹D. Faiman, H. J. Lipkin, and H. Rubinstein, Phys. Lett. **59B**, 269 (1975).

²⁰If we neglect the pion mass and take $b = 0$, Table I implies

$$\frac{\Gamma(f_0 \rightarrow \gamma\gamma)}{\Gamma(f_0 \rightarrow \pi\pi)} = \frac{200}{243} \frac{\alpha^2}{(g_\rho^2/4\pi)^2},$$

as found in Ref. 19. When $a = 0$ this ratio becomes instead

$$\frac{\Gamma(f_0 \rightarrow \gamma\gamma)}{\Gamma(f_0 \rightarrow \pi\pi)} = \frac{81}{400} \frac{\alpha^2}{(g_\rho^2/4\pi)^2},$$

a value 6 times larger than the value for $b = 0$. The value in Eq. (46) implies an even larger ratio as a result of the destructive interference between a and b in $f_0 \rightarrow \pi\pi$. These effects were anticipated to some extent in Ref. 19.

²¹J. Rosner, in *Electromagnetic and Weak Interactions*, Proceedings of the VIII Rencontre de Moriond, Méribel-Iles-Allues, France, 1973, edited by J. Tran Thanh Van (Université de Paris-Sud, Orsay, 1973), p. 29.

²²In Ref. 14 it was mentioned that the results of applying the Melosh approach to the decay $f_0 \rightarrow \gamma\gamma$ were still unknown, and could differ from the " I -broken SU(6)_W" used in Ref. 21. The results of Table I in fact turn out to be *identical* to those obtained from " I -broken SU(6)_W."

²³The " I -broken SU(6)_W" approach for relating electromagnetic decays to pionic decays is described by W. P. Petersen and J. L. Rosner, Phys. Rev. D **7**, 747 (1973). This approach was motivated by the same quark-pair-creation picture taken earlier for the description of pionic decays alone (see Ref. 14).

²⁴H. Kastrup, Nucl. Phys. B**15**, 179 (1970); L. N. Chang and P. G. O. Freund, Ann. Phys. (N.Y.) **61**, 182 (1970); R. Crewther, Phys. Rev. D **3**, 3152 (1971), **4**, 3814 (E) (1971).

²⁵B. Gobbi, J. L. Rosen, H. A. Scott, S. L. Shapiro, L. Strawczynski, and C. M. Meltzer, Phys. Rev. Lett. **33**, 1450 (1974): $\Gamma(\rho^- \rightarrow \pi^- \gamma) = 35 \pm 10$ keV.

²⁶W. C. Carithers, P. Mühlemann, D. Underwood, and D. G. Ryan, Phys. Rev. Lett. **35**, 349 (1975): $\Gamma(K^*0 \rightarrow K^0 \gamma) = 75 \pm 35$ keV.

²⁷P. J. O'Donnell, Phys. Rev. Lett. **36**, 177 (1976).

²⁸H. Primakoff, Phys. Rev. **81**, 899 (1951).

²⁹See Sec. 3.3.4 of Ref. 14 for a discussion. In that reference the factors $(\frac{2}{3})^{1/2}$ in Eqs. (56) and (57) were inadvertently omitted, leading to erroneous predictions for $\Gamma(\eta' \rightarrow \gamma\gamma)$ and $\Gamma(\eta \rightarrow \gamma\gamma)$.

³⁰M. Chanowitz, Phys. Rev. Lett. **35**, 977 (1975), discusses the experimental implications of this ratio from a different point of view.

³¹A. Kotlewski, W. Lee, M. Suzuki, and J. Thaler, Phys. Rev. D **8**, 348 (1973).

³²A. Browman *et al.*, Phys. Rev. Lett. **32**, 1067 (1974).

³³R. Hofstadter, Ann. Rev. Nucl. Sci. **7**, 231 (1957).

³⁴Hey *et al.*, Ref. 2.

³⁵See, e.g., S. J. Brodsky, T. Kinoshita, and H. Terazawa, Phys. Rev. D 4, 1532 (1971).

³⁶G. Masek, private communication.

³⁷B. Schrempp-Otto, F. Schrempp, and T. F. Walsh, Phys. Lett. 36B, 463 (1971). For a related approach with very different conclusions, see A. Bramón and M. Greco, Lett. Nuovo Cimento 2, 522 (1971).

³⁸B. Renner, Nucl. Phys. B30, 634 (1971). For further refinements and a discussion of the possibility that $\Gamma(\epsilon \rightarrow \gamma\gamma) = 0$ see H. Kleinert, L. P. Staunton, and P. H.

Weisz, Nucl. Phys. B38, 87 (1972).

³⁹P. Grassberger and R. Kögerler, Nucl. Phys. B106, 451 (1976).

⁴⁰For a prediction of small a/b based on the application of duality to $B \rightarrow \omega\pi$, see H. Haut, Phys. Rev. D 10, 3097 (1974). A particular dual amplitude used by N. Levy, P. Singer, and S. Toaff, Phys. Rev. D 13, 2662 (1976), also entails definite $f\rho\rho$ couplings. These authors compare their predictions [$\Gamma(f \rightarrow \gamma\gamma) \cong 5$ keV, $\Gamma(f \rightarrow \rho\gamma) \cong 0.6$ MeV] with those of a number of other authors.